3. Zhang B, Liu S, Tan T, et al. Treatment with convalescent plasma for critically ill patients with SARS-CoV-2 infection. *Chest*. 2020;158(1):e9-e13.

4. Dzik S. COVID-19 convalescent plasma: now is the time for better science. *Transfus Med Rev*. 2020;34(3):141-144.

5. Ye M, Fu D, Ren Y, et al. Treatment with convalescent plasma for COVID-19 patients in Wuhan, China. *J Med Virol*. 2020;92(10):1890-1901.

6. Zeng Q-L, Yu Z-J, Gou J-J, et al. Effect of convalescent plasma therapy on viral shedding and survival in COVID-19 patients. *J Infect Dis*. 2020;222(1): 38-43.

7. Hegerova L, Gooley TA, Sweerus KA, et al. Use of convalescent plasma in hospitalized patients with COVID-19: case series. *Blood*. 2020;136(6): 759-762.

8. Rojas M, Rodríguez Y, Monsalve DM, et al. Convalescent plasma in COVID-19: possible mechanisms of action. *Autoimmun Rev*. 2020;19(7):102554.

9. Rajendran K, Krishnasamy N, Rangarajan J, et al. Convalescent plasma transfusion for the treatment of COVID-19: systematic review. *J Med Virol*. 2020;92:1475-1483.

10. Gharbharan A, Jordans CCE, Geurtsvankessel C. Convalescent plasma for COVID-19. A randomized clinical trial [published online ahead of print 3 July 2020]. *medRxiv*. doi:10.1101/2020.07.01.20139857.

11. Li L, Zhang W, Hu Y, et al. Effect of convalescent plasma therapy on time to clinical improvement in patients with severe and life-threatening COVID-19: a randomized clinical trial. *JAMA*. 2020;324(5):460-470.

12. Ni L, Ye F, Cheng M-L, et al. Detection of SARS-CoV-2-specific humoral and cellular immunity in COVID-19 convalescent individuals. *Immunity*. 2020;52(6):971-977.e3.

13. Wu F, Wang A, Liu M, et al. Neutralizing antibody responses to SARS-CoV-2 in a COVID-19 recovered patient cohort and their implications [published online ahead of print 20 April 2020]. *medRxiv*. doi:10.1101/2020.03.30.20047365.

14. Jackson LA, Anderson EJ, Rouphael NG, et al; mRNA-1273 Study Group. An mRNA vaccine against SARS-CoV-2: preliminary report [published online ahead of print 14 July 2020]. *N Engl J Med*. doi:10.1056/NEJMoa2022483.

15. Beaudoin-Bussières G, Laumaea A, Anand SP, et al. Decline of humoral responses against SARS-CoV-2 spike in convalescent Individuals. *mBio*. 2020;11(5):e02590-20.

16. Prévost J, Gasser R, Beaudoin-Bussières G, et al. Cross-sectional evaluation of humoral responses against SARS-CoV-2 spike. *Cell Rep Med*. 2020;1(7):100126.

17. Zhang G, Nie S, Zhang Z, Zhang Z. longitudinal change of severe acute respiratory syndrome coronavirus 2 antibodies in patients with coronavirus disease 2019. *J Infect Dis*. 2020;222(2):183-188.

18. Long Q-X, Liu B-Z, Deng H-J, et al. Antibody responses to SARS-CoV-2 in patients with COVID-19. *Nat Med*. 2020;26(6):845-848.

19. Lynch KL, Whitman JD, Lacanienta NP, et al. Magnitude and kinetics of anti-SARS-CoV-2 antibody responses and their relationship to disease severity. *Clinical Infectious Diseases*. 2020;ciaa979.

20. Long Q-X, Tang X-J, Shi Q-L, et al. Clinical and immunological assessment of asymptomatic SARS-CoV-2 infections. *Nat Med*. 2020;26(8):1200-1204.

21. Seow J, Graham C, Merrick B, et al. Longitudinal evaluation and decline of antibody responses in SARS-CoV-2 infection [published online ahead of print 11 July 2020]. *medRxiv*. doi:10.1101/2020.07.09.20148429.

22. Wang K, Long Q-X, Deng H-J, et al. Longitudinal dynamics of the neutralizing antibody response to SARS-CoV-2 infection. *Clin Infect Dis*. 2020; ciaa1143.

23. Morell A, Terry WD, Waldmann TA. Metabolic properties of IgG subclasses in man. *J Clin Invest*. 1970;49(4):673-680.

24. Amanna IJ, Slifka MK. Mechanisms that determine plasma cell lifespan and the duration of humoral immunity. *Immunol Rev*. 2010;236(1):125-138.

25. Sekine T, Perez-Potti A, Rivera-Ballesteros O, et al; Karolinska COVID-19 Study Group. Robust T cell immunity in convalescent individuals with asymptomatic or mild COVID-19. *Cell*. 2020;183(1):158-168.

26. Woloshin S, Patel N, Kesselheim AS. False negative tests for SARS-CoV-2 infection—challenges and implications. *N Engl J Med*. 2020;383:e38.

27. Mallapaty S. Will coronavirus antibody tests really change everything? *Nature*. 2020;580:571-572.

28. Xia X, Li K, Wu L, et al. Improved clinical symptoms and mortality among patients with severe or critical COVID-19 after convalescent plasma transfusion. *Blood*. 2020;136(6):755-759.

DOI 10.1182/blood.2020008367

TO THE EDITOR:

MPN patients with low mutant *JAK2* allele burden show late expansion restricted to erythroid and megakaryocytic lineages

Ronny Nienhold,[1] Peter Ashcroft,[2] Jakub Zmajkovic,[1] Shivam Rai,[1] Tata Nageswara Rao,[1] Beatrice Drexler,[3] Sara C. Meyer,[1,3] Pontus Lundberg,[1,3] Jakob R. Passweg,[3] Danijela Leković,[4] Vladan Čokić,[5] Sebastian Bonhoeffer,[2] and Radek C. Skoda[1]

[1]Department of Biomedicine, University Hospital Basel and University of Basel, Basel, Switzerland; [2]Institute of Integrative Biology, Eidgenössische Technische Hochschule (ETH) Zürich, Zürich, Switzerland; [3]Division of Hematology, University Hospital Basel, Basel, Switzerland; [4]Clinic of Hematology, Clinical Center of Serbia, Belgrade, Serbia; and [5]Institute for Medical Research, University of Belgrade, Belgrade, Serbia

Myeloproliferative neoplasms (MPNs) are clonal hematopoietic stem cell (HSC) diseases characterized by increased proliferation of erythroid, megakaryocytic, and/or myeloid lineages.[1] The *JAK2*-V617F mutation can be found in >95% of polycythemia vera (PV) patients, and also in approximately one-half of patients with essential thrombocythemia (ET) or primary myelofibrosis (PMF).[2-5] Somatic mutations in exon 12 of *JAK2* are found in 3% to 5% of PV patients.[6] Quantification of the *JAK2*-mutant allele burden, also called variant allele frequency (VAF), in DNA from peripheral blood granulocytes is used to monitor the size of the mutant clone. ET patients have lower *JAK2* VAF than PMF or PV patients.[7] Interestingly, some MPN patients display very low VAF, which calls into question why they develop MPNs if the clone is apparently unable to expand. We therefore studied MPN patients with *JAK2* VAF ≤20%.

In our cohort of 205 patients with *JAK2*-V617F$^+$ MPNs, we identified 56 patients with a VAF ≤20% in purified granulocyte

DNA (supplemental Figure 1A, available on the *Blood* Web site). Survival of MPN patients with low *JAK2*-V617F VAF was not significantly altered compared with other MPN patients (supplemental Figure 1B-D). The contribution of the *JAK2*-mutant clone to peripheral blood lineages was previously shown to be highly variable between individual MPN patients,[8,9] and low VAF correlated with lineage-restricted clonal distribution.[9] We therefore determined the *JAK2* VAF in platelets and reticulocytes, representing the lineages most relevant to ET and PV, respectively. The purification procedures are described in supplemental Figures 2 and 3. Because platelets and reticulocytes do not contain DNA, we established a quantitative polymerase chain reaction assay to measure *JAK2*-V617F in RNA (supplemental Figure 2C).

RNA from purified platelets was available from 44 of 56 patients (79%) with low *JAK2*-V617F VAF (supplemental Figure 4). One patient (P021) simultaneously also carried a *JAK2* exon 12 mutation and we included 2 additional patients with a *JAK2* exon 12 mutation in our study. Most patients with ET and PMF, as well as 15 of 17 patients with PV (88%), had higher *JAK2* VAF in platelets compared with granulocytes (Figure 1A). We were able to obtain fresh blood and to purify reticulocytes by fluorescence-activated cell sorting (FACS) from 22 of 46 patients (48%) with available platelet RNA. All patients with PV and PMF and, surprisingly, 8 of 11 patients with ET (72%) had higher *JAK2* VAF in reticulocytes compared with granulocytes (Figure 1B). This increase in allele burden compared with granulocytes was restricted to platelets and reticulocytes (Figure 1C). We can distinguish 4 patterns of lineage contribution of the *JAK2*-mutant clone (Figure 1D): a "platelet-biased" pattern, with increased mutant allele burden solely in platelets; a "red cell–biased" pattern, with a selective increase in reticulocytes; a "platelet and red cell–biased" pattern, with increase in both platelets and reticulocytes; and a "persistently low" pattern, with very low allele burden in granulocytes, platelets, and reticulocytes.

To define at which stages of the hematopoietic development the expansion of the *JAK2*-mutant clone occurs, we determined the *JAK2* VAF by genotyping single myeloid and erythroid progenitors (Figure 2A; supplemental Figure 5). As expected, the derived VAF in granulocyte and granulocyte/monocyte colonies (colony-forming unit granulocyte/granulocyte-macrophage [CFU-G/GM]) was low and comparable with VAF in peripheral blood granulocytes. Burst-forming unit–erythroid (BFU-E) colonies also showed very low VAF, but, in most patients, VAF substantially increased in peripheral blood reticulocytes, suggesting that the expansion of the mutant clone occurs at late stages of erythroid development. The late erythroid expansion of the *JAK2*-mutant clone in PV patients could be favored by low serum erythropoietin levels and hypersensitivity of *JAK2*-V617F–expressing progenitors to erythropoietin.[10]

To complement the data from single colonies, we isolated megakaryocyte progenitors (MkPs) and other progenitor cell populations from peripheral blood by FACS (supplemental Figure 6). Consistent with the data obtained in the analysis of single colonies, in the vast majority of patients, the *JAK2*-mutant VAF was low in MkPs and other sorted progenitor subsets (Figure 2B; supplemental Figure 7). In contrast, a large percentage of erythroid progenitors was positive for the *JAK2* mutation in previous reports, when patients with higher *JAK2* allele burden were analyzed.[9,11,12] Thus, the expansion of the *JAK2*-mutant clone at terminal stages of erythroid and/or megakaryocytic development appears to be typical for the low allele burden subset of MPN patients (Figure 2C).

Lineage-biased HSCs and long-term progenitors have been described.[13-16] We hypothesized that MPN patients with low VAF might acquire the *JAK2* mutation in such progenitors and we expected that single platelet-biased or red cell–biased patterns would be the most frequent. However, our data do not favor such a model. The frequent occurrence of the platelet and red cell–biased pattern in MPN patients with low VAF fits with the proposed model of a "biological continuum" between the phenotypes of *JAK2*-V617F^{+} ET and PV.[17] However, none of the PV or ET patients with low VAF displayed a dominant homozygous subclone (supplemental Figure 5), which is typically found in the majority of PV patients.[11,12,18]

To examine the role of additional somatic mutations, we analyzed 104 cancer-related genes using targeted next-generation sequencing.[19] Additional somatic mutations were detected in 12 of the 46 patients with low VAF (26%) (supplemental Figure 8; supplemental Table 1). The presence of additional somatic mutations had no relevant impact on the mutant allele distributions (supplemental Figure 8D). We determined the clonal architecture in 11 of 12 patients with additional somatic gene mutations by genotyping single hematopoietic colonies (supplemental Figure 8E). A sequential pattern of acquisition of mutations was observed in 4 of 11 patients (36%). In all of these patients, the additional somatic mutation was acquired before *JAK2*-V617F. In the remaining 7 patients (64%), a biclonal pattern was observed, with the *JAK2* mutation and the additional somatic gene mutation representing separate clones. Thus, interestingly, none of the patients with low VAF displayed *JAK2* mutation as the first event, and the frequency of the biclonal pattern appears to be higher than the reported frequency of 30% in overall MPNs.[19,20]

To derive hypotheses that could explain the observed clonal structures, we generated an online app based on a compartmental mathematical model of hematopoiesis (https://ibz-shiny.ethz.ch/ashcroft/lowJAK2/app/; supplemental Methods). This model approximates the continuous process of hematopoietic development and assumes that the cells in each compartment are homogeneous and indistinguishable. All analysis is based on the steady state of the system.[21-23] The dynamics of cells in each compartment can be described by 4 parameters: self-renewal probability (a_i), division rate (b_i), lineage bias (c_{ij}), and probability of death (d_i) (Figure 2D). The influence of independently varying the mutant's parameters on the mutant allele burden is summarized in supplemental Figure 9. By modifying the parameters at different stages of hematopoietic development, we can qualitatively reproduce all observed patterns of clonal expansion in MPN patients with low VAF (Figure 2E; supplemental Figure 10). We therefore hypothesize that interindividual differences in these 4 parameters are sufficient to explain the different patterns of mutant allele burden observed in MPN patients. Indeed, differences in expression levels of JAK2 and MPL protein have been shown to determine thrombopoietin-induced megakaryocyte proliferation vs differentiation,[24] and, on mouse models, resulted in switching between ET and PV phenotypes.[25] Additional factors contributing to interindividual differences in

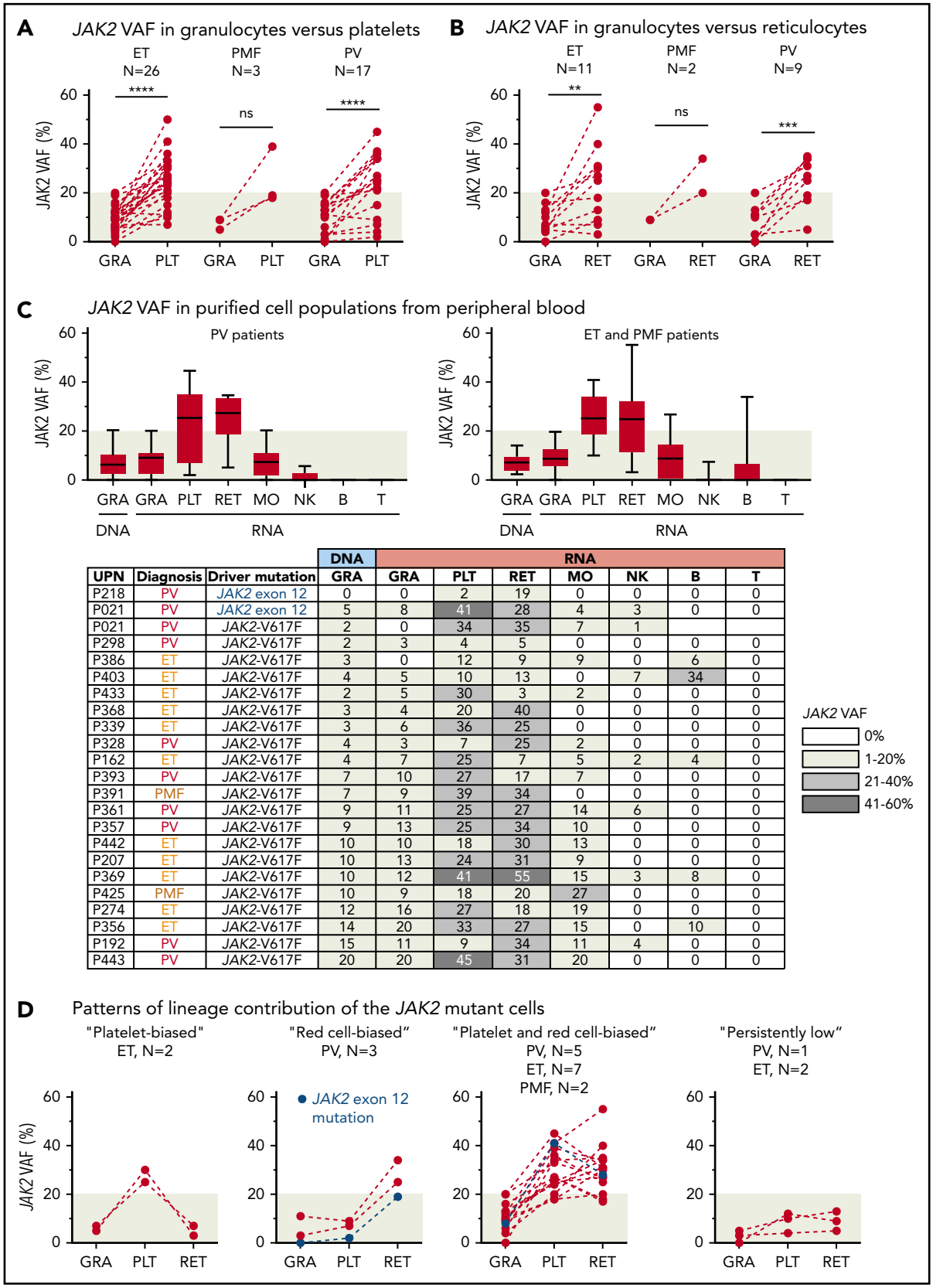

			DNA	RNA						
UPN	Diagnosis	Driver mutation	GRA	GRA	PLT	RET	MO	NK	B	T
P218	PV	*JAK2* exon 12	0	0	2	19	0	0	0	0
P021	PV	*JAK2* exon 12	5	8	41	28	4	3	0	0
P021	PV	*JAK2*-V617F	2	0	34	35	7	1		
P298	PV	*JAK2*-V617F	2	3	4	5	0	0	0	0
P386	ET	*JAK2*-V617F	3	0	12	9	9	0	6	0
P403	ET	*JAK2*-V617F	4	5	10	13	0	7	34	0
P433	ET	*JAK2*-V617F	2	5	30	3	2	0	0	0
P368	ET	*JAK2*-V617F	3	4	20	40	0	0	0	0
P339	ET	*JAK2*-V617F	3	6	36	25	0	0	0	0
P328	PV	*JAK2*-V617F	4	3	7	25	2	0	0	0
P162	ET	*JAK2*-V617F	4	7	25	7	5	2	4	0
P393	PV	*JAK2*-V617F	7	10	27	17	7	0	0	0
P391	PMF	*JAK2*-V617F	7	9	39	34	0	0	0	0
P361	PV	*JAK2*-V617F	9	11	25	27	14	6	0	0
P357	PV	*JAK2*-V617F	9	13	25	34	10	0	0	0
P442	ET	*JAK2*-V617F	10	10	18	30	13	0	0	0
P207	ET	*JAK2*-V617F	10	13	24	31	9	0	0	0
P369	ET	*JAK2*-V617F	10	12	41	55	15	3	8	0
P425	PMF	*JAK2*-V617F	10	9	18	20	27	0	0	0
P274	ET	*JAK2*-V617F	12	16	27	18	19	0	0	0
P356	ET	*JAK2*-V617F	14	20	33	27	15	0	10	0
P192	PV	*JAK2*-V617F	15	11	9	34	11	4	0	0
P443	PV	*JAK2*-V617F	20	20	45	31	20	0	0	0

Figure 1. Analysis of *JAK2* VAFs in peripheral blood. (A) Comparison of *JAK2* VAF measured in RNA from granulocytes (GRA) vs platelets (PLT). Dashed lines connect data points from the same patient. (B) Comparison of *JAK2* VAF measured in RNA from granulocytes vs reticulocytes (RET). (C) *JAK2* VAF in purified cell populations from peripheral blood. Boxes represent 50% of the measured values; whiskers indicate the range; and horizontal lines indicate the median. The *JAK2* VAF of 22 patients measured in DNA or RNA from different peripheral blood lineages is shown below. Numbers in the cells of the table indicate the percentages of *JAK2* VAF; the shading of boxes corresponds to the ranges shown on the right. (D) Patterns of lineage contribution of the *JAK2*-mutant cells derived from the data presented in panels A and B. $^{**}P < .01$; $^{***}P < .001$; $^{****}P < .0001$. B, B cell; MO, monocyte; NK, natural killer cell; ns, not significant; T, T cell; UPN, unique patient number.

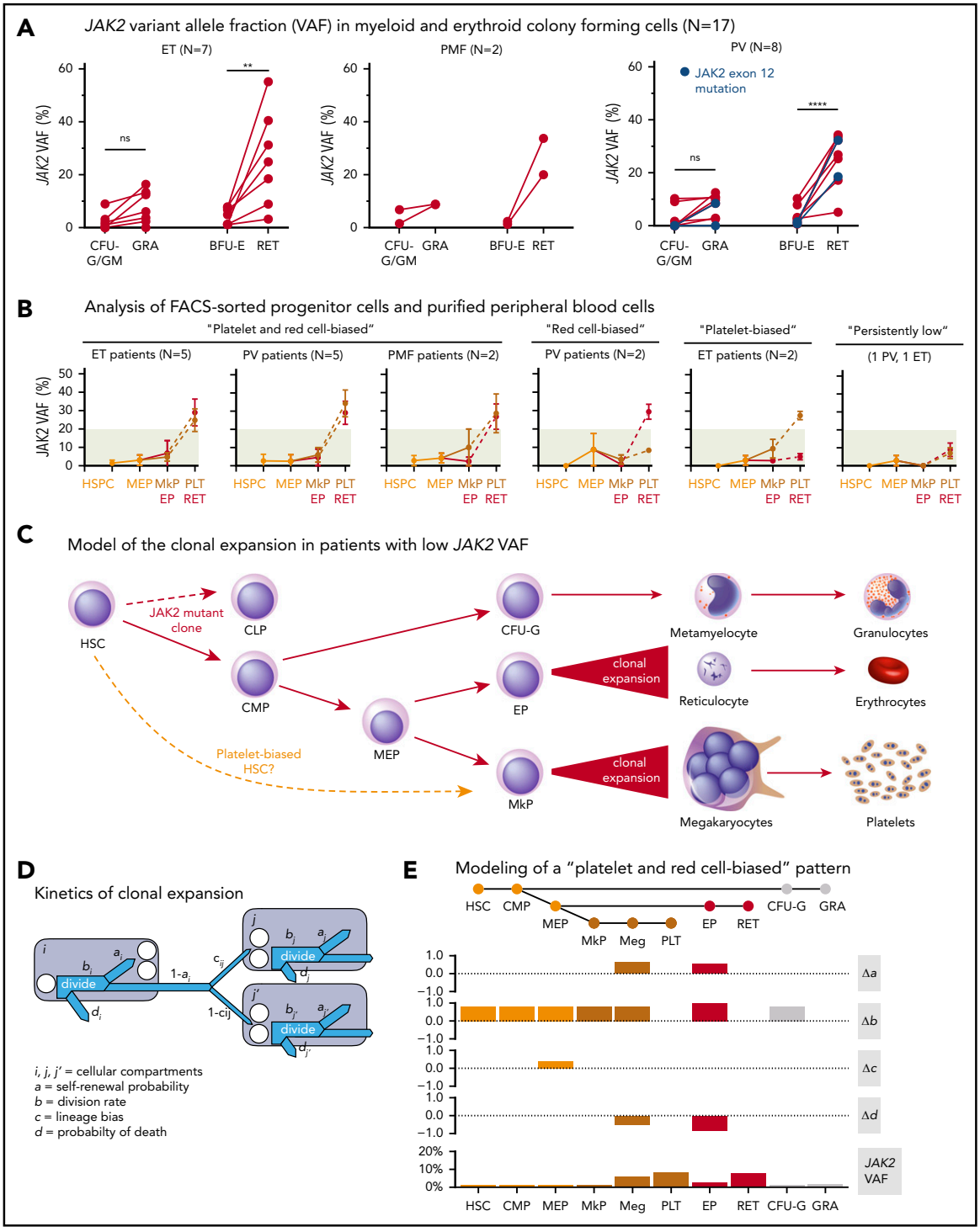

Figure 2. Analysis of *JAK2* VAFs in hematopoietic progenitors. (A) Analysis of single colonies grown in methylcellulose. Single erythroid colonies (burst-forming unit–erythroid [BFU-E]) and granulocyte or granulocyte/monocyte colonies (colony-forming unit granulocyte/granulocyte-macrophage [CFU-G/GM]) were picked, and the percentage of *JAK2*-mutant colonies was converted into VAF by taking into account the heterozygous and homozygous state of each colony. (B) *JAK2* VAF in FACS-sorted progenitor cells and mature blood cells. Data from 17 MPN patients are shown. Data points connected by solid lines were obtained from FACS-sorted progenitor cells. Dashed lines connect the progenitors with their corresponding mature cells isolated from peripheral blood. (C) Model depicting the stages of hematopoiesis in which the clonal expansion occurred in MPN patients with low *JAK2* VAF. (D) Schematic illustration of dynamics in a branched population structure. (E) Modeling of a common platelet and red cell–biased pattern using the branched compartmental model of hematopoiesis. The distribution of *JAK2*-mutant cells observed in MPN patients with low VAF can be reproduced by altering the division rate (*b*), self-renewal (*a*), and death (*d*) probabilities, and the differentiation bias (*c*) at specific stages of hematopoietic development. For the clonal expansion during terminal stages of megakaryopoiesis, Δa signifies the probability that megakaryocytes repeatedly undergo endomitosis resulting in higher ploidy, and the division rate Δb stands for the number of endomitoses per time unit, for example, per day. Hematopoietic cell compartments are indicated on the x-axis. $^{**}P < .01$; $^{****}P < .0001$. CLP, common lymphoid progenitor; CMP, common myeloid progenitor; EP, erythroid progenitor; HSPC, hematopoietic stem and progenitor cell; Meg, megakaryocyte; MEP, megakaryocyte-erythroid progenitor.

humans could be the availability and activity of downstream signaling components and differences in genetic background.

Acknowledgments

The authors thank Nils Hansen for helpful comments on the manuscript. The authors also thank Hui Hao-Shen, Gabriele Mild-Schneider, and Hélène Mereau for valuable technical support; Danny Labes and Emmanuel Traunecker for cell sorting; Christian Beisel, Genomics Facility Basel, for conducting next-generation sequencing; and Susanne Erpel, Nano Imaging Laboratory, Swiss Nanoscience Institute (SNI), University of Basel, for performing the scanning electron microscopy.

This work was supported by grants from the Swiss Cancer League (KLS-2950-02-2012 and KFS-3655-02-2015), SystemsX.ch (Medical Research and Development grant 2014/266), and the Swiss National Science Foundation (31003A-147016/1 and 31003A_166613) (R.C.S.) and from the Swiss National Science Foundation through a joint research project (SCOPES IZ73Z0 152420/1; V.C. and R.C.S.).

Authorship

Contribution: R.N. performed research, analyzed data, and wrote the manuscript; P.A. and S.B. analyzed data and performed mathematical modeling; J.Z. and S.R. performed research; T.N.R. designed research; B.D., S.C.M., J.R.P., D.L., and V.C. collected data; P.L. designed research and analyzed data; and R.C.S. designed research, analyzed data, and wrote the manuscript.

Conflict-of-interest disclosure: The authors declare no competing financial interests.

ORCID profiles: R.N., 0000-0001-5057-430X; P.A., 0000-0003-4067-7692; T.N.R., 0000-0002-9928-5944; J.R.P., 0000-0001-7092-3351; D.L., 0000-0002-6194-8298; V.C., 0000-0002-0362-1449; S.B., 0000-0001-8052-3925.

Correspondence: Radek C. Skoda, Department of Biomedicine, University Hospital Basel and University of Basel, Hebelstrasse 20, Basel, 4031 Switzerland; e-mail: radek.skoda@unibas.ch.

Footnotes

Submitted 5 February 2020; accepted 9 July 2020; prepublished online on *Blood* First Edition 22 July 2020.

For original data, please e-mail the corresponding author, Radek C. Skoda, at radek.skoda@unibas.ch.

The online version of this article contains a data supplement.

REFERENCES

1. Barbui T, Thiele J, Gisslinger H, et al. The 2016 WHO classification and diagnostic criteria for myeloproliferative neoplasms: document summary and in-depth discussion. *Blood Cancer J*. 2018;8(2):15.
2. Kralovics R, Passamonti F, Buser AS, et al. A gain-of-function mutation of JAK2 in myeloproliferative disorders. *N Engl J Med*. 2005;352(17):1779-1790.
3. Levine RL, Wadleigh M, Cools J, et al. Activating mutation in the tyrosine kinase JAK2 in polycythemia vera, essential thrombocythemia, and myeloid metaplasia with myelofibrosis. *Cancer Cell*. 2005;7(4):387-397.
4. James C, Ugo V, Le Couédic JP, et al. A unique clonal JAK2 mutation leading to constitutive signalling causes polycythaemia vera. *Nature*. 2005;434(7037):1144-1148.
5. Baxter EJ, Scott LM, Campbell PJ, et al; Cancer Genome Project. Acquired mutation of the tyrosine kinase JAK2 in human myeloproliferative disorders. *Lancet*. 2005;365(9464):1054-1061.
6. Scott LM, Tong W, Levine RL, et al. JAK2 exon 12 mutations in polycythemia vera and idiopathic erythrocytosis. *N Engl J Med*. 2007;356(5):459-468.
7. Passamonti F, Rumi E, Pietra D, et al. Relation between JAK2 (V617F) mutation status, granulocyte activation, and constitutive mobilization of CD34+ cells into peripheral blood in myeloproliferative disorders. *Blood*. 2006;107(9):3676-3682.
8. Bellosillo B, Martínez-Avilés L, Gimeno E, et al. A higher JAK2 V617F-mutated clone is observed in platelets than in granulocytes from essential thrombocythemia patients, but not in patients with polycythemia vera and primary myelofibrosis. *Leukemia*. 2007;21(6):1331-1332.
9. Li S, Kralovics R, De Libero G, Theocharides A, Gisslinger H, Skoda RC. Clonal heterogeneity in polycythemia vera patients with JAK2 exon12 and JAK2-V617F mutations. *Blood*. 2008;111(7):3863-3866.
10. Dupont S, Massé A, James C, et al. The JAK2 617V>F mutation triggers erythropoietin hypersensitivity and terminal erythroid amplification in primary cells from patients with polycythemia vera. *Blood*. 2007;110(3):1013-1021.
11. Scott LM, Scott MA, Campbell PJ, Green AR. Progenitors homozygous for the V617F mutation occur in most patients with polycythemia vera, but not essential thrombocythemia. *Blood*. 2006;108(7):2435-2437.
12. Godfrey AL, Chen E, Pagano F, Silber Y, Campbell PJ, Green AR. Clonal analyses reveal associations of JAK2V617F homozygosity with hematologic features, age and gender in polycythemia vera and essential thrombocythemia. *Haematologica*. 2013;98(5):718-721.
13. Yamamoto R, Morita Y, Ooehara J, et al. Clonal analysis unveils self-renewing lineage-restricted progenitors generated directly from hematopoietic stem cells. *Cell*. 2013;154(5):1112-1126.
14. Sanjuan-Pla A, Macaulay IC, Jensen CT, et al. Platelet-biased stem cells reside at the apex of the haematopoietic stem-cell hierarchy. *Nature*. 2013;502(7470):232-236.
15. Haas S, Hansson J, Klimmeck D, et al. Inflammation-induced emergency megakaryopoiesis driven by hematopoietic stem cell-like megakaryocyte progenitors. *Cell Stem Cell*. 2015;17(4):422-434.
16. Nishikii H, Kanazawa Y, Umemoto T, et al. Unipotent megakaryopoietic pathway bridging hematopoietic stem cells and mature megakaryocytes. *Stem Cells*. 2015;33(7):2196-2207.
17. Campbell PJ, Scott LM, Buck G, et al; Australasian Leukaemia and Lymphoma Group. Definition of subtypes of essential thrombocythaemia and relation to polycythaemia vera based on JAK2 V617F mutation status: a prospective study. *Lancet*. 2005;366(9501):1945-1953.
18. Godfrey AL, Chen E, Pagano F, et al. JAK2V617F homozygosity arises commonly and recurrently in PV and ET, but PV is characterized by expansion of a dominant homozygous subclone. *Blood*. 2012;120(13):2704-2707.
19. Lundberg P, Karow A, Nienhold R, et al. Clonal evolution and clinical correlates of somatic mutations in myeloproliferative neoplasms. *Blood*. 2014;123(14):2220-2228.
20. Kent DG, Ortmann CA, Green AR. Effect of mutation order on myeloproliferative neoplasms. *N Engl J Med*. 2015;372(19):1865-1866.
21. Marciniak-Czochra A, Stiehl T, Ho AD, Jäger W, Wagner W. Modeling of asymmetric cell division in hematopoietic stem cells--regulation of self-renewal is essential for efficient repopulation. *Stem Cells Dev*. 2009;18(3):377-385.
22. Stiehl T, Marciniak-Czochra A. Characterization of stem cells using mathematical models of multistage cell lineages. *Math Comput Model*. 2011;53(7-8):1505-1517.
23. Rodriguez-Brenes IA, Komarova NL, Wodarz D. Evolutionary dynamics of feedback escape and the development of stem-cell-driven cancers. *Proc Natl Acad Sci USA*. 2011;108(47):18983-18988.
24. Besancenot R, Roos-Weil D, Tonetti C, et al. JAK2 and MPL protein levels determine TPO-induced megakaryocyte proliferation vs differentiation. *Blood*. 2014;124(13):2104-2115.
25. Tiedt R, Hao-Shen H, Sobas MA, et al. Ratio of mutant JAK2-V617F to wild-type Jak2 determines the MPD phenotypes in transgenic mice. *Blood*. 2008;111(8):3931-3940.

DOI 10.1182/blood.2019002943

Supplemental Methods

Patient cohort

Blood samples and clinical data of MPN patients were collected at the University Hospital Basel, Switzerland and at the Clinical Center of Serbia, Belgrade, Serbia. The study was approved by the local Ethics Committees (Ethik Kommission Beider Basel and Ethics commissions of Clinical Center of Serbia and Institute for Medical Research, University of Belgrade, Belgrade). Written informed consent was obtained from all patients in accordance with the Declaration of Helsinki. The diagnosis of MPN was established according to the 2016 revision of the World Health Organization classification of myeloid neoplasms and acute leukemia.[1,2]

Isolation of individual cell types

Fresh peripheral blood was centrifuged to separate platelet-rich plasma from white and red blood cells. Platelets were isolated from platelet-rich plasma by Sepharose chromatography and purity was determined by an ADVIA120 Hematology Analyzer using Multispecies Version 5.9.0-MS software (Bayer, Supplemental Figure S2C). Fractions of peripheral blood mononuclear cells (PBMCs), granulocytes and red cells were separated by density centrifugation using Lymphoprep (by Axis-Shield). PBMCs and granulocytes were treated with red cell lysis buffer (0.15 M NH4Cl, 0.01 M KHCO3, 0.05 M EDTA, pH8). Reticulocytes were enriched from the erythrocyte fraction using CD71 MicroBeads (130-046-201, Miltenyi Biotec) and further purified by FACS sorting using the following antibodies: PE/Cy7 anti-human CD45 (304016, Biolegend), APC anti-human CD71 (334108, Biolegend), Pacific Blue anti-human CD235a (349108, Biolegend) and PE anti-human CD42a (558819, BD Biosciences). Monocytes, NK-cells, B- and T-cells were purified by FACS sorting from PBMCs using the following antibodies: PE anti-human CD335 (331908, Biolegend), BV421 anti-human CD3 (317344, Biolegend), APC anti-human CD14 (325608, Biolegend) and FITC anti-human CD19 (302206, Biolegend). The progenitors were purified by FACS sorting from PBMCs using the following antibodies: BV786 anti-human CD45RA (563870, BD Biosciences), APC-H7 anti-human CD71 (563671, BD Biosciences), PerCP/Cy5.5 anti-human CD105 (323215, Biolegend), FITC anti-human lineage cocktail (348701, Biolegend), BV605 anti-human CD123 Antibody (306025, Biolegend), SYTOX Dead Cell Stain (S34860, Thermo Fisher Scientific),

PE anti-human CD42a (558819, BD Biosciences), Pacific Blue anti-human CD34 (343512, Biolegend) and APC anti-human CD38 (356606, Biolegend). The gating strategies are depicted in Supplemental Figure 3A-D.[3]

DNA from granulocytes was extracted with Qiamp DNA mini kit (Qiagen). RNA from granulocytes and platelets was extracted using Trifast Peq Gold (PEQLAB Biotechnologie). RNA from sorted cells was extracted by PicoPure RNA Isolation Kit (Thermo Fisher Scientific).

Quantification of *JAK2*-V617F and *JAK2*-exon 12 variant allele fraction (VAF)

An allele-specific polymerase chain reaction (AS-PCR) was performed for the detection of *JAK2*-V617F in genomic DNA.[4] The SNaPshot Multiplex Kit (Applied Biosystems) was applied for the detection of the *JAK2*-V617F mutation in RNA samples and the detection of *JAK2*-exon12 mutations in DNA and RNA.[4,5] The primers for these analyses are shown below.

List of primers used in the study	Assay	Primer ID	Primer sequence (5'-3')
Quantification of JAK2-V617F in DNA	asPCR	Jak2-V617F-RT	6Fam-AAATTACTCTCGTCTCCACAGAA
		Jak2-V617F-F	GTTTCTTAGTGCATCTTTATTATGGCAGA
		Jak2-V617F-RG	6Fam-TTACTCTCGTCTCCACAGAC
Amplification of JAK2 exon 14 from DNA	SNaPshot assay	4586_hJak2_intron13_fwd	AGAATTTTCTGAACTATTTATGG
		4587_hJak2_intron14_rev	ACCTAGCTGTGATCCTGAAACTG
Amplification of JAK2 exon 14 from RNA	SNaPshot assay	4336_hJAK2-ex13-fwd	GGCGTACGAAGAGAAGTAG
		4337_hJAK2-ex15-rev	GCCCATGCCAACTGTTTA
Quantification of JAK2-V617F	SNaPshot assay	4338_hJAK2-VF-SNaP-fwd	AAGCATTTGGTTTTAAATTATGGAGTATGT
Amplification of JAK2 exon 12 from DNA	SNaPshot assay	2075_hJAK2-exon12-F	CAAAGTTCAATGAGTTGACCCC
		2076_hJAK2-exon12-R	TGCTAACATCTAACACAAGGTTGG
Amplification of JAK2 exon 12 from RNA	SNaPshot assay	4416_hJAK2-exon11-fwd	ACTAAATGCTGTCCCCCAAA
		4417_hJAK2-exon13-rev	TACTTCTCTTCGTACGCCTT
Quantification of JAK2-exon12 (P021)	SNaPshot assay	4420_P021del_SNPsht_fwd	AAAGTCTGACAACAAATGGTGTTTCACAAAATCAGA
Quantification of JAK2-exon12 (P218)	SNaPshot assay	4426_P216aaTT_SNPsht_rev	TAGGTAAATATCAAATCTTCATTTCTGATT

The amplicons generated by AS-PCR or SNaPshot Multiplex Kit were analyzed with an ABI3130xl Genetic Analyzer (Applied Biosystems Inc.). The VAF was calculated by Peak height$_{mut}$ / (Peak height$_{mut}$ + Peak height$_{wt}$) x 100 %.

Next-generation sequencing analyses

To detect additional somatic mutations, DNA from granulocytes was analyzed with a targeted NGS approach covering the coding regions of 104 genes, as previously published.[6] For library preparation, 500 ng of genomic DNA from granulocytes was fragmented by ultrasonic sheering (Covaris) and barcoded using NEXTflex Rapid DNA Sequencing Kit and barcodes (BiooScientific). Agilent SureSelect custom design was used for the capture of target regions. Paired-end 100-bp cycle sequencing of the captured libraries was performed using an Illumina HiSeq2000. CLC genomics workbench was used for mapping of the raw reads and variant calling.

Methylcellulose assay

The colony assays were performed using peripheral blood mononuclear cells from patients as previously published.[7] In brief, PBMCs were seeded in methylcellulose (H4034, StemCell technologies) and cultured at 37°C and 5% CO_2. After 14 days, colonies were picked for DNA extraction and analyzed individually for *JAK2*-V617F using AS-PCR and for the presence of somatic mutations by Sanger sequencing, respectively. On average, 178 colonies per patient were analyzed. To determine the temporal order of mutation acquisition, at least 2 informative colonies were required.

Statistical analysis

Statistical significance of the data was tested with one-way ANOVA or two-way ANOVA and analyzed using GraphPad Prism 7 software with the following significance levels: $p<0.05$= *, $p<0.01$= ** and $p<0.001$= ***.

Mathematical modeling

A simple compartmental model is used that is based on existing models of hierarchical tissue structures.[8-10] In such a model, cells are assigned into one of a number of compartments based on their phenotype, with stem cells (HSCs) occupying the first compartment ($i = 1$). Each compartment i contains a number of cells, which we write as x_i. The parameter set $\{a_i, b_i, c_{ij}, d_i\}$ determines the dynamics of the cells in each compartment in the following way:

1. A cell in compartment i is chosen to divide with rate b_i (per unit time);
2. With probability d_i, the chosen cell dies and is lost from the population;
3. If the chosen cell survives, then with probability a_i it generates two daughter cells that remain in the same compartment (self-renewal);
4. With probability $1 - a_i$, the daughter cells are differentiated from the parent;
5. Of these differentiated cells, a fraction c_{ij} transform into type-j cells. This parameter represents the differentiation bias of the type-i cells. If $c_{ij} = 1$, then only type-j cells can be produced when i differentiates. If $c_{ij} = 0$, then type-j cells cannot be produced by i.

These dynamics are highlighted in the Figure 1 below.

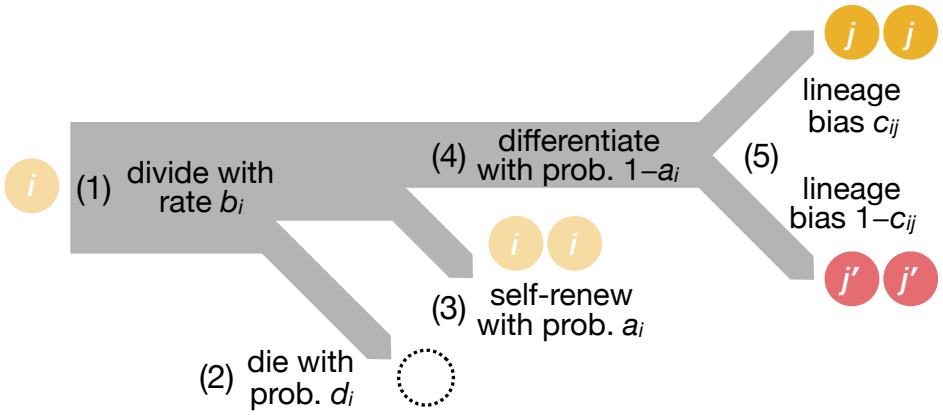

Figure 1: Cell dynamics schematic

The *JAK2*-V617F clone follows the same dynamical structure, but parameters may be different from those of the wild-type. Each compartment i has y_i mutant cells, and their dynamics are described by the parameter set $\{a_i', b_i', c_{ij}', d_i'\}$. For simplicity, we assume there is no interaction between the wildtype and mutant cells. The dynamical equations for this process are then given by

$$\dot{x}_i = 2\sum_j b_j(1-d_j)(1-a_j)c_{ji}x_j - b_i[1-2a_i(1-d_i)]x_i, \#(1a)$$

$$\dot{y}_i = 2\sum_j b_j'(1-d_j')(1-a_j')c_{ji}'y_j - b_i'[1-2a_i'(1-d_i')]y_i. \#(1b)$$

These equations permit the steady state (x_i^*, y_i^*). Note that $a_1(1-d_1) = a_1'(1-d_1') = 0.5$ is required for the steady-state to exist. We then investigate how changes to the mutant-specific parameters alter the variant allele fraction (VAF) when the system has reached its steady state. This VAF is defined as the fraction of mutant cells in a given compartment:

$$z_i = \frac{y_i^*}{x_i^* + y_i^*}.$$

If the parameters of the mutant cells are identical to the WT, i.e. $a_i' = a_i$, $b_i' = b_i$, $c_{ij}' = c_{ij}$, and $d_i' = d_i$ for all i, j, then VAF is preserved from the HSCs such that $z_i \equiv z_1$ for all i. Varying the mutant's parameters from the WT's, however, will change the VAF across the compartments. Below we consider the VAF response to changes in a single parameter from $\{a_i', b_i', c_{ij}', d_i'\}$. In Figures 2E, S9 and S10, the parameter change from WT to mutant is represented as the fractional difference, e.g. $\Delta a_i = (a_i' - a_i)/a_i$.

Varying division rates: Increasing the division rate of the mutant in a single downstream compartment (b_i for $i > 1$) will decrease the VAF observed in that compartment, but will remain unchanged elsewhere (Figure S9B, left panel). If the mutant HSC division rate (b_1) is increased, then the mutant VAF increases in all downstream compartments, while it remains constant in the HSCs. Combining these two observations, a late clonal expansion can be observed by in compartment i by increasing division rates b_j for all compartments j upstream of i (Figure S9B, right panel).

Varying death rate: Decreasing the probability that a mutant cell dies in compartment i (d_i) leads to an increase VAF in that compartment, and an even greater increase in VAF in downstream compartments (Figure S9C, left panel). Late clonal expansions can then be observed if the final mutant progenitor cells are less likely to die (Figure S9C, right panel).

Varying self-renewal probabilities: If the mutants have an increased probability to self-renew in compartment i, then the mutant VAF will increase in that compartment as well as in downstream compartments, although to a lesser extent (Figure S9D, left panel). Late clonal expansions can then be observed if the final mutant progenitor cells are more likely to self-renew (Figure S9D, right panel).

Varying lineage bias: The impact of modifying the lineage bias of mutant cells c'_{ij} is quite predictable: If mutant cells are more prone to differentiating into one lineage, then the VAF will increase in that lineage and decrease in the other. This is shown in Figure S9F.

Finally, we comment on the assumptions of the model. The compartmentalized view of hematopoiesis that we employ here is an approximation of the continuous process – in reality cell phenotypes can take in infinite number of values. The discrete models reflect the classical treatment of phenotype data, where cells are clustered into compartments based on properties such as surface-marker or RNA expression. Bridging the gap between the discrete and continuum views of hematopoiesis is an emerging direction of research, but it has been shown that a suitable choice of

differentiation rate function in the continuous model can reproduce exactly the dynamics of the discrete model.[11-12] Therefore, we can say our results are robust to the choice of modelling framework.

We also provide an online app for the mathematical modeling that can be used to test various settings of the parameters and observe the resulting alterations in the variant allele frequencies that are predicted to occur:
https://ibz-shiny.ethz.ch/ashcroft/lowJAK2/app/
The code archive can be found at: https://www.doi.org/10.5281/zenodo.3900156

Supplemental References

1. Arber DA, Orazi A, Hasserjian R, et al. The 2016 revision to the World Health Organization classification of myeloid neoplasms and acute leukemia. *Blood*. 2016;127(20):2391-2405.
2. Thiele J, Kvasnicka HM, Orazi A, et al. Myeloprolifierative Neoplasms. In: Swerdlow SH, Campo E, Harris NL, et al., eds. WHO Classification of Tumours of Haematopoietic and Lymphoid Tissues. Lyon: International Agency for Research on Cancer (IARC); 2017:585.
3. Miyawaki K, Iwasaki H, Jiromaru T, et al. Identification of unipotent megakaryocyte progenitors in human hematopoiesis. *Blood*. 2017;129(25):3332-3343.
4. Kralovics R, Teo SS, Li S, et al. Acquisition of the V617F mutation of JAK2 is a late genetic event in a subset of patients with myeloproliferative disorders. *Blood*. 2006;108(4):1377-1380.
5. Li S, Kralovics R, De Libero G, Theocharides A, Gisslinger H, Skoda RC. Clonal heterogeneity in polycythemia vera patients with JAK2 exon12 and JAK2-V617F mutations. *Blood*. 2008;111(7):3863-3866.
6. Lundberg P, Karow A, Nienhold R, et al. Clonal evolution and clinical correlates of somatic mutations in myeloproliferative neoplasms. *Blood*. 2014;123(14):2220-2228.
7. Schaub FX, Jager R, Looser R, et al. Clonal analysis of deletions on chromosome 20q and JAK2-V617F in MPD suggests that del20q acts independently and is not one of the predisposing mutations for JAK2-V617F. *Blood*. 2009;113(9):2022-2027.
8. Marciniak-Czochra A, Stiehl T, Ho AD, Jager W, Wagner W. Modeling of asymmetric cell division in hematopoietic stem cells--regulation of self-renewal is essential for efficient repopulation. *Stem Cells Dev*. 2009;18(3):377-385.
9. Stiehl T, Marciniak-Czochra A. Characterization of stem cells using mathematical models of multistage cell lineages. *Mathematical and Computer Modelling*. 2011;53(7-8):1505-1517.
10. Rodriguez-Brenes IA, Komarova NL, Wodarz D. Evolutionary dynamics of feedback escape and the development of stem-cell-driven cancers. *Proc Natl Acad Sci U S A*. 2011;108(47):18983-18988.
11. Doumic M, Marciniak-Czochra A, Perthame B, Zubelli JP. A structured population model of cell differentiation. *SIAM J. Appl. Math.* 2011;71(6):1918-1940.
12. Gwiazda P, Jamróz G, Marciniak-Czochra A. Models of discrete and continuous cell differentiation in the framework of transport equation. *SIAM J. Appl. Math.* 2012;44(2):1103-1133.

Supplemental Figure S1

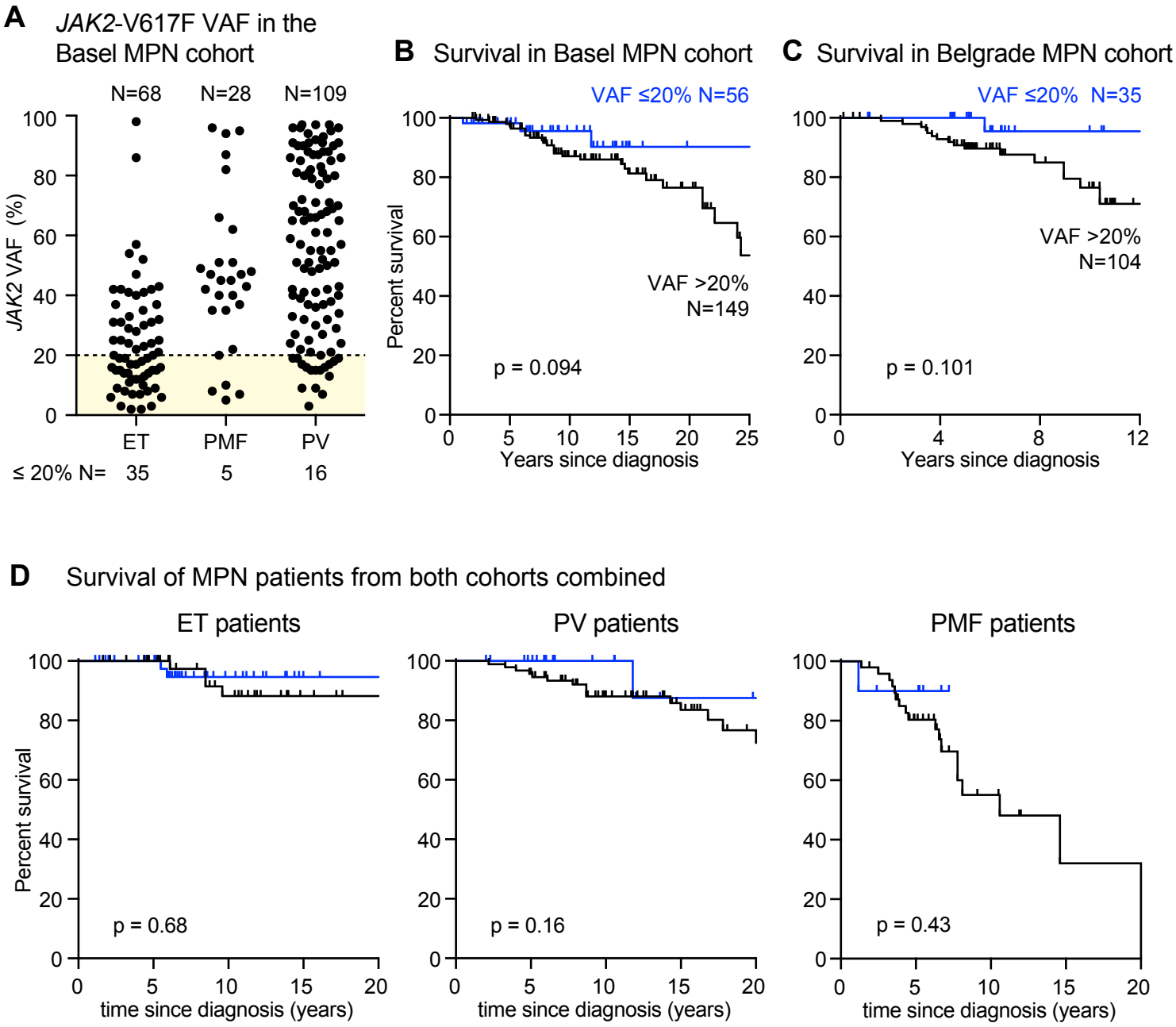

Supplemental Figure S1: A) *JAK2*-V617F variant allele fraction (VAF) in granulocyte DNA in the Basel cohort of MPN patients. ET, essential thrombocythemia, PV, polycythemia vera, PMF, primary myelofibrosis. Patients with *JAK2* VAF ≤ 20% (yellow box) were selected for further analysis. B) Survival of patients from the Basel cohort with low mutant allele burden depicted as a Kaplan-Meier plot (p values determined by log-rank Mantel-Cox test). C) Survival of patients with low *JAK2* VAF from a second independent cohort of MPN patients. D) Survival for individual MPN subentities. Patients from both cohorts were combined and are plotted separately for each MPN subentity.

Supplemental Figure S2

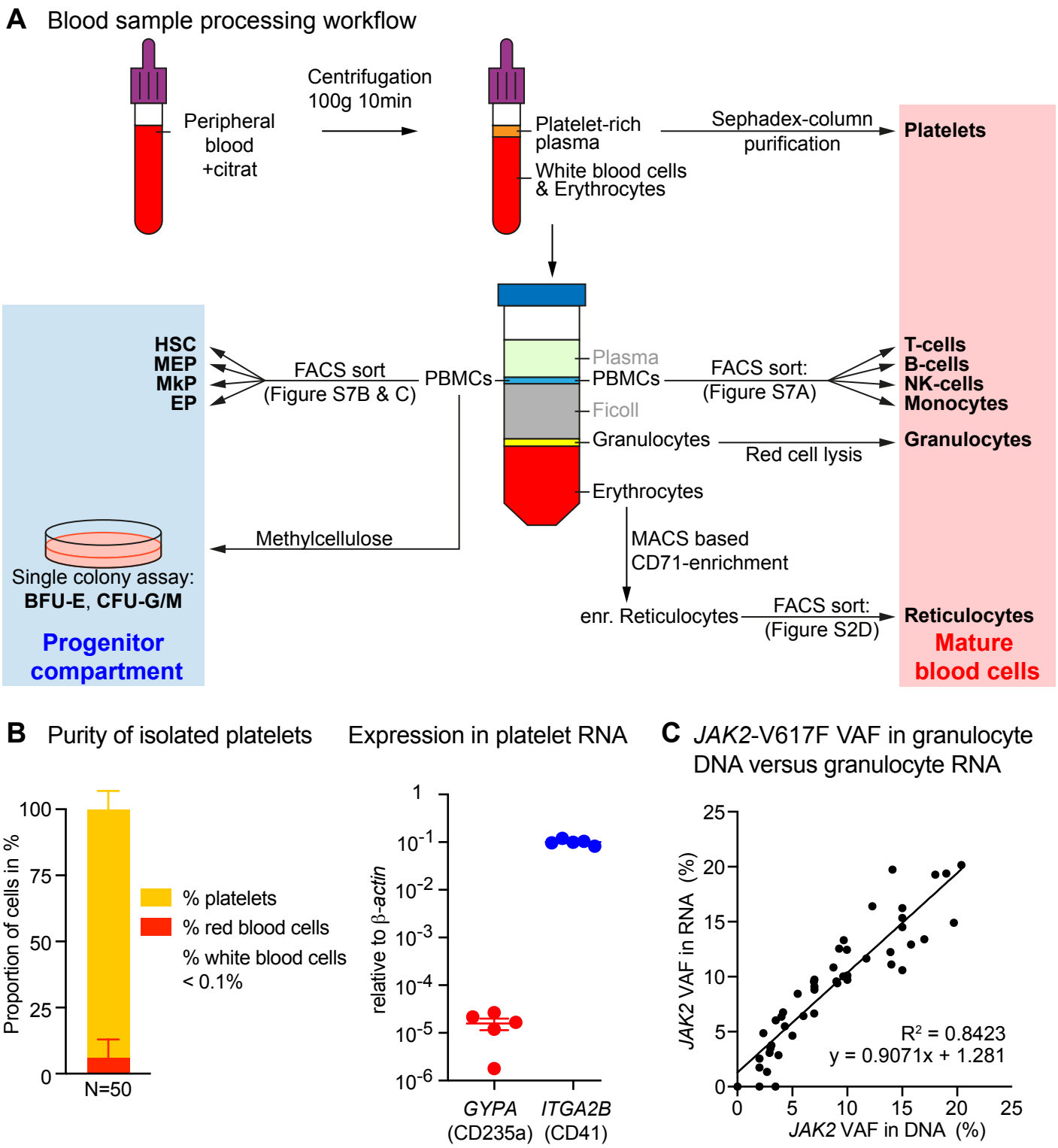

Supplemental Figure S2: A) Workflow for the processing of peripheral blood samples. B) Purity of platelets measured prior to RNA extraction, measured with the ADVIA120 Hematology Analyzer and expression of *glycophorin A* (*GYPA,* CD235a) and *ITGA2B* (CD41) in platelet mRNA determined by qPCR. Values relative to β-*actin* are shown on a logarithmic scale. C) Correlation of allele burden measured in DNA and RNA extracted from purified granulocytes of patients with a low *JAK2*-V617F variant allele fraction (VAF).

Supplemental Figure S3

A Sorting of reticulocytes from CD71-enriched red cell fraction

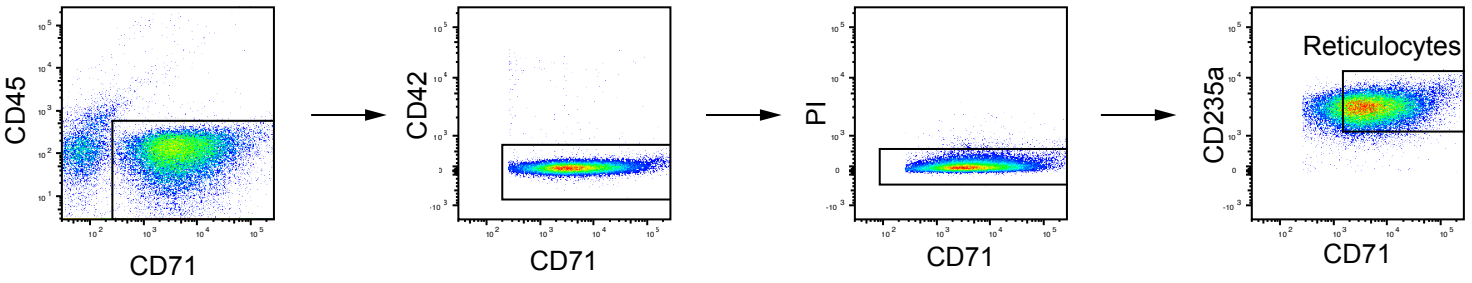

B Reanalysis of sorted reticulocytes

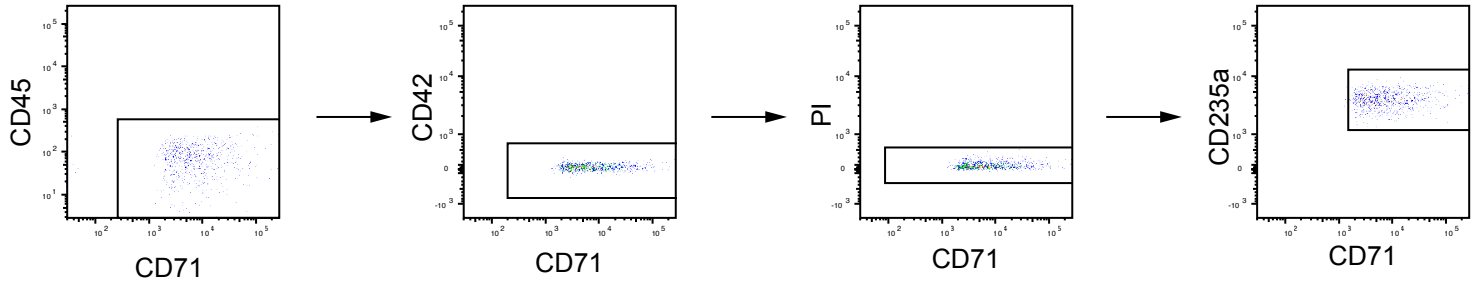

C Sorting of Monoctytes, NK-cells, B-cells and T-cells from peripheral blood mononuclear cells

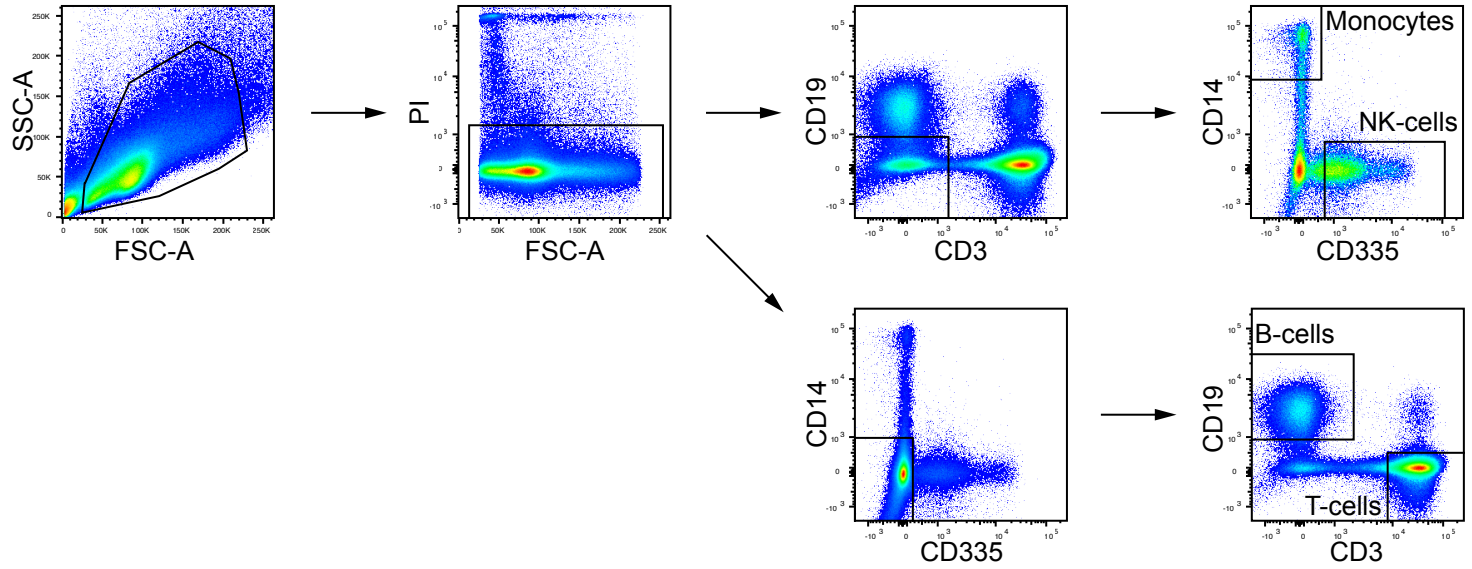

Supplemental Figure S3: Gating strategy for sorting of cell populations from peripheral blood. A and B) Strategy for sorting and reanalyzing reticulocytes from CD71-enriched red cell fraction from peripheral blood. C) Sorting of white blood cell lineages from peripheral blood mononuclear cells.

Supplemental Figure S4

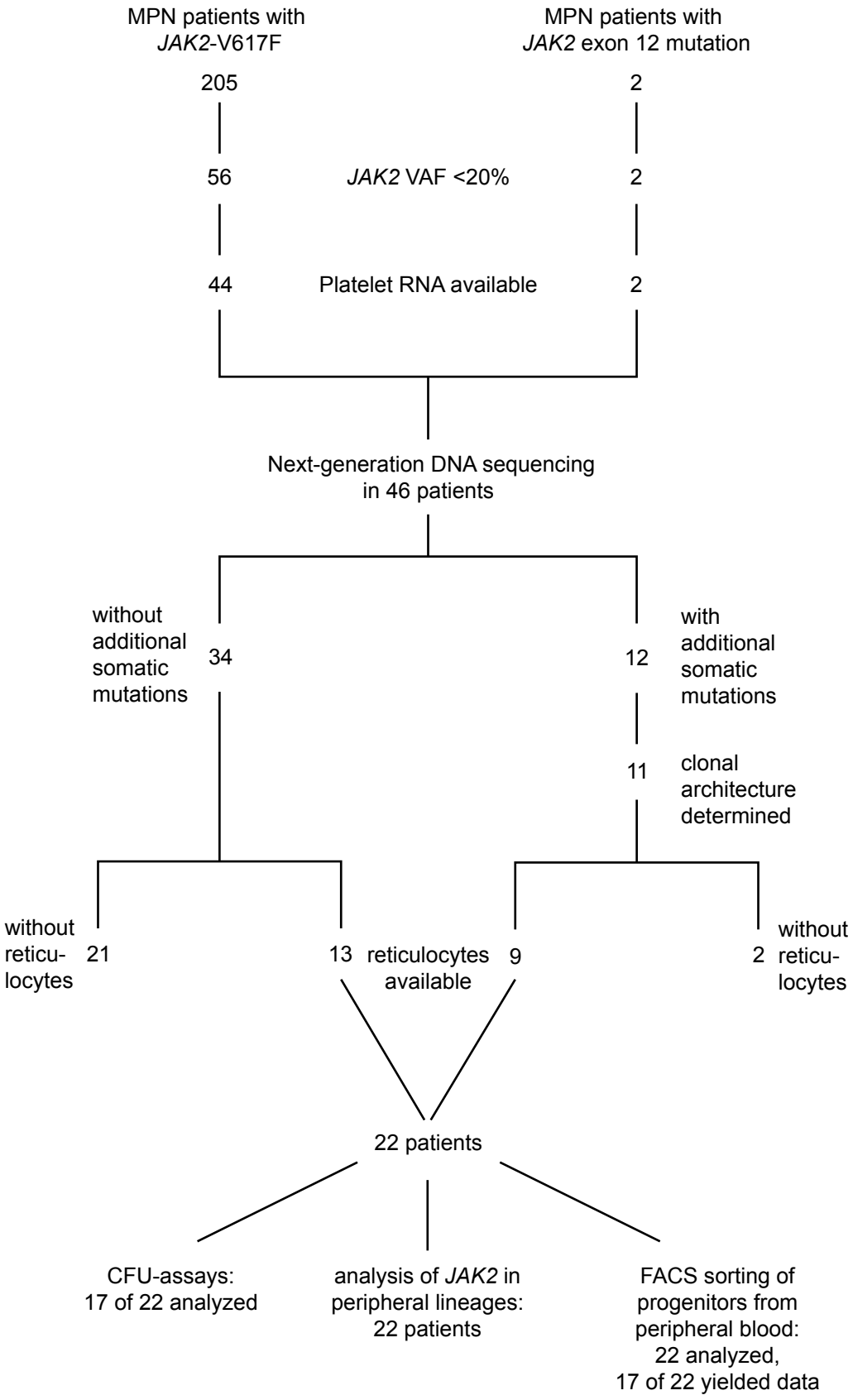

Supplemental Figure S4: Flow chart of patients included in the study. VAF, variant allele fraction. Numbers of patients included and procedures that were performed are shown.

Supplemental Figure S5

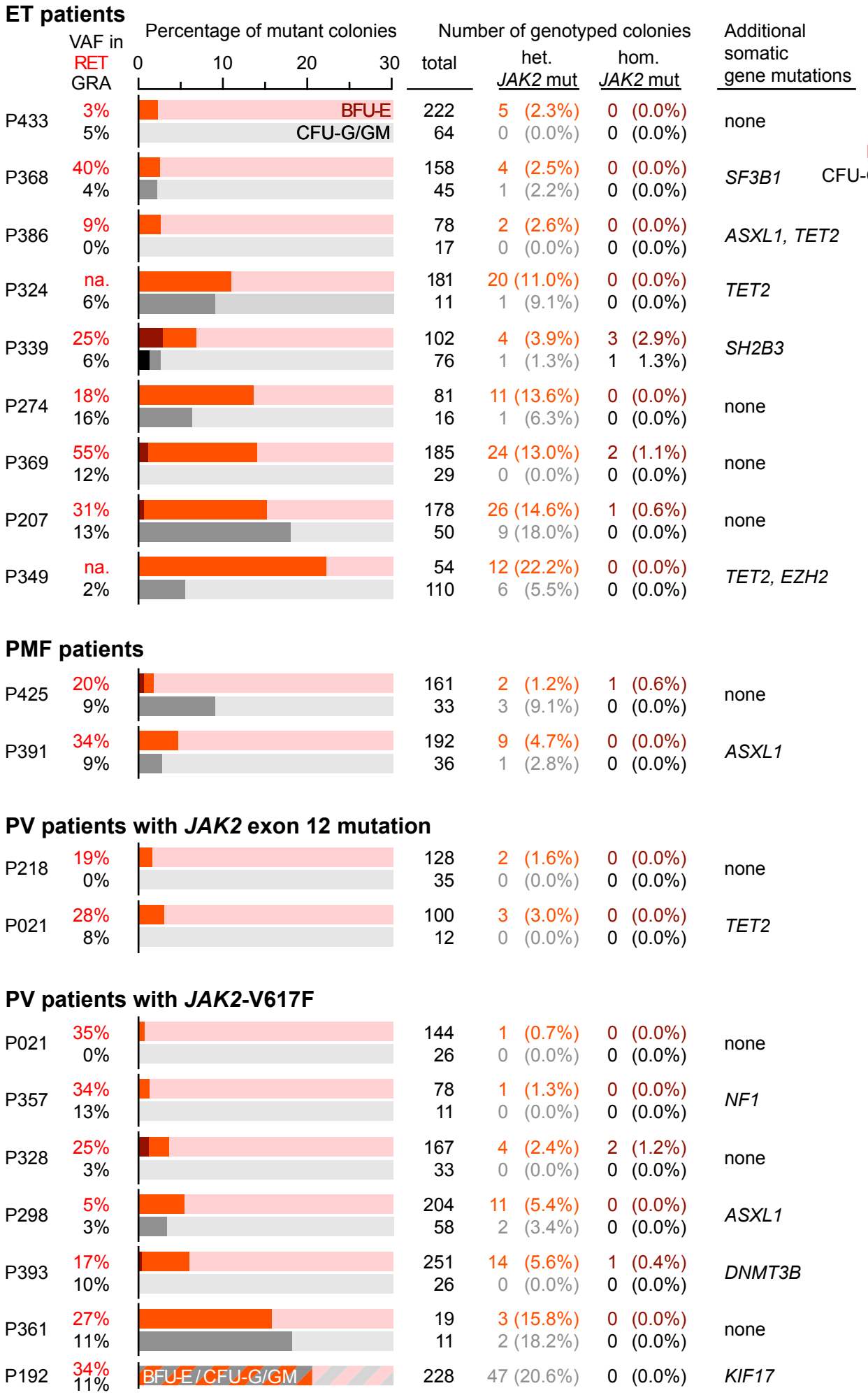

Supplemental Figure S5: Summary of analyses on single colonies grown in methylcellulose. Bars show the relative frequency of *JAK2*-mutated bust forming unit-erythroid (BFU-E) and colony forming unit-granulocyte/ granulocyte-monocyte (CFU-G/GM) colonies. VAF, *JAK2* variant allele fraction in reticulocytes (RET) and granulocytes (GRA); hom, homozygous; het, heterozygous; WT, wildtype.

Supplemental Figure S6

A Sorting of hematopoietic progenitors from peripheral blood of P328

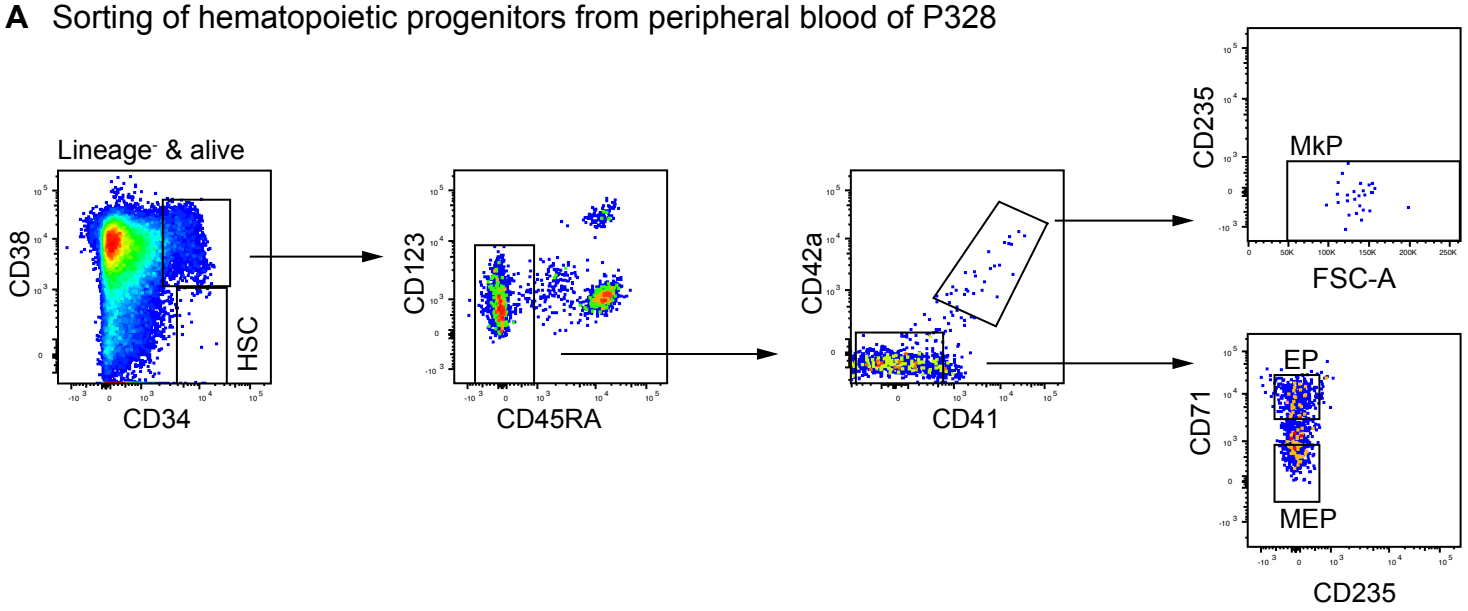

B Sorting of hematopoietic progenitors from bone marrow of P368

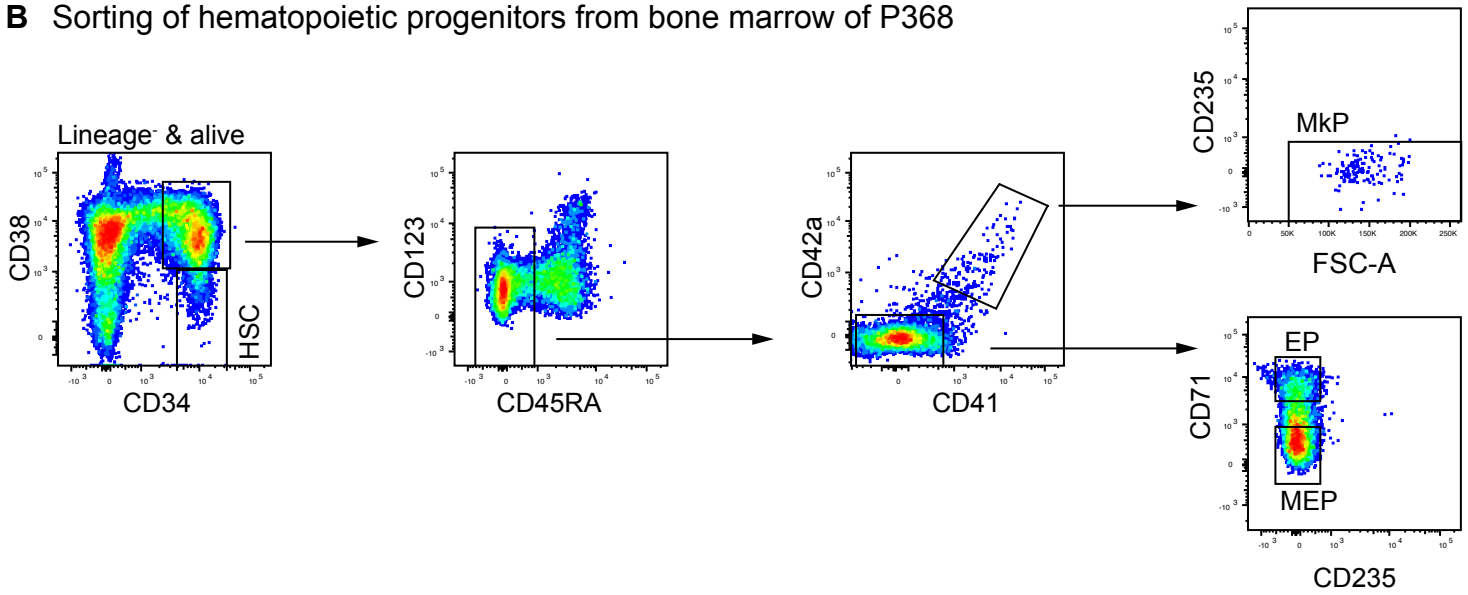

Supplemental Figure S6: Gating strategy for the sorting of hematopoietic progenitors. A) Sorting of peripheral blood mononuclear cells. B) Sorting of bone marrow cells. HSC, hematopoietic stem cell; MEP, megakaryocyte erythroid progenitor; MkP, megakaryocyte progenitor; EP, erythroid progenitor cells.

Supplemental Figure S7

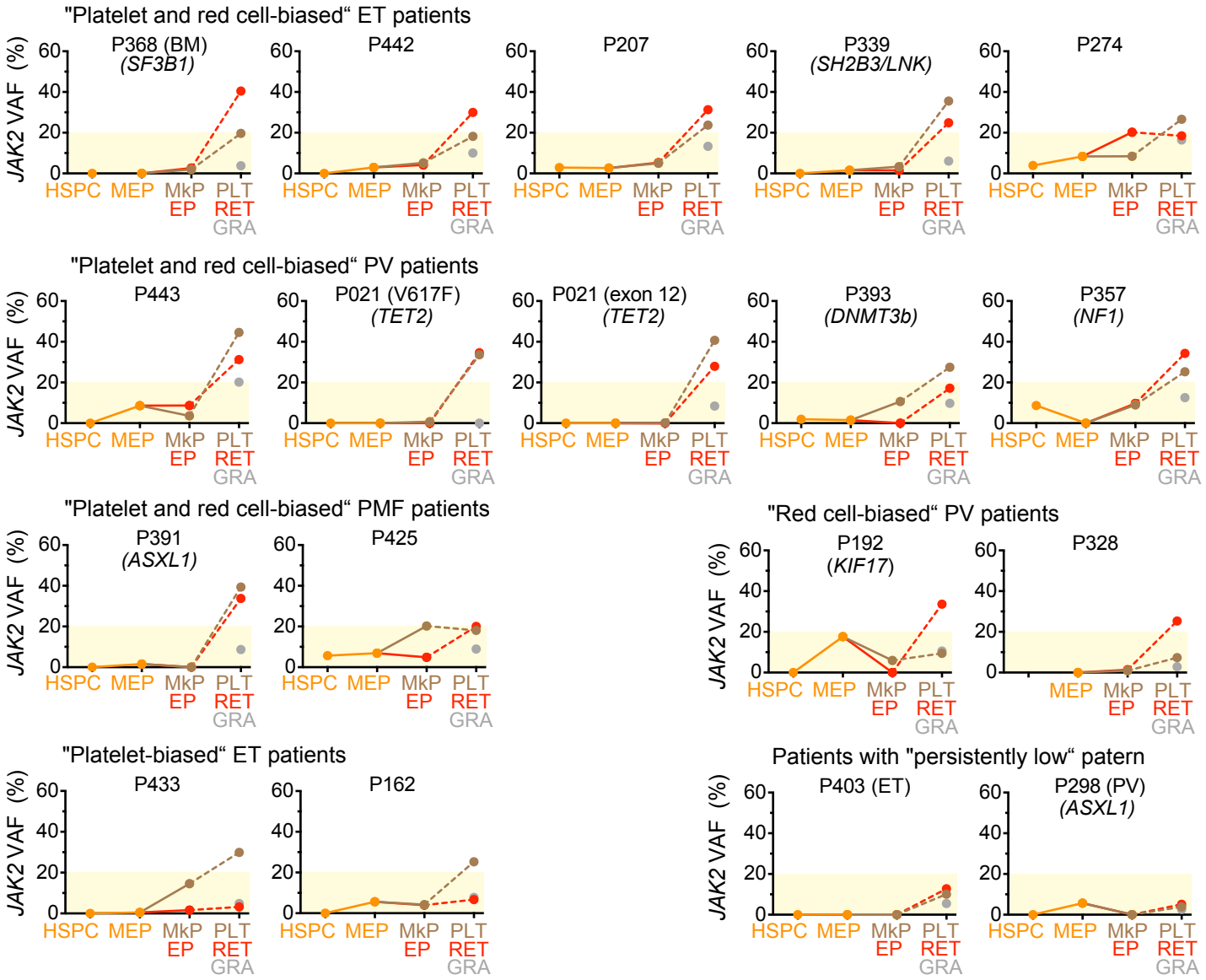

Supplemental Figure S7: *JAK2* variant allele fraction (VAF) in FACS-sorted progenitor cells and mature blood cells. Data of 17 individual MPN patients are shown. Cells from bone marrow (BM) were analyzed in one patient (P368), all other analyses were performed on cells from peripheral blood. Data points connected by solid lines were obtained from FACS-sorted progenitor cells. Dashed lines connect the progenitors with their corresponding mature cells isolated from peripheral blood. HSPC, hematopoietic stem and progenitor cells; MEP, megakaryocyte-erythroid progenitors; MkP, megakaryocytic progenitors; EP, erythroid progenitors.

Supplemental Figure S8

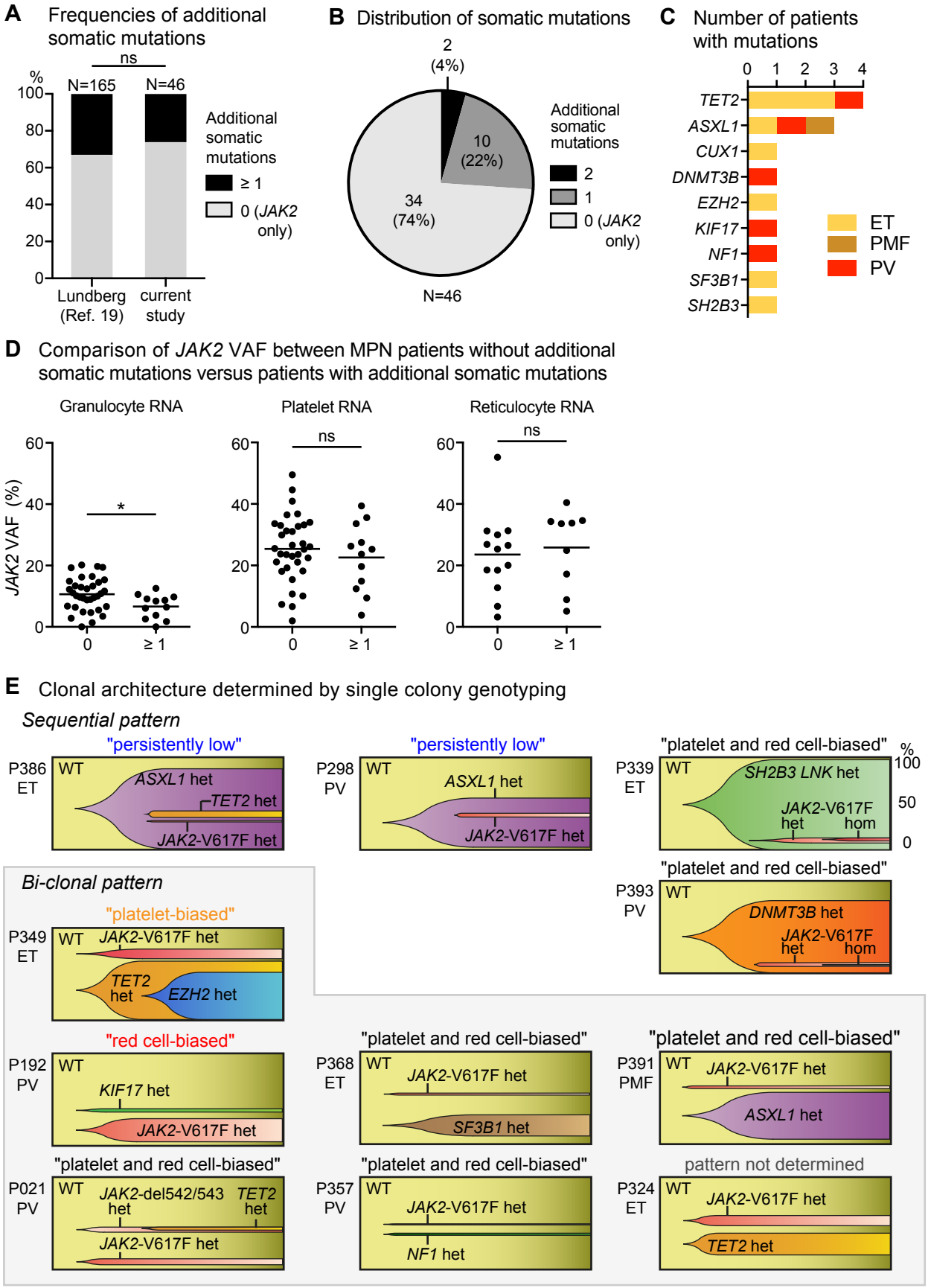

Supplemental Figure S8: Mutation profiles of MPN patients with low *JAK2* variant allele fraction (VAF). A) Proportions of patients with additional somatic mutations from a previously published cohort of *JAK2*-V617F mutant patients and the 46 patients with low *JAK2* VAF. B) Distribution of additional somatic mutations detected by targeted next generation sequencing. C) Number of patients with mutations in the indicated genes. D) Distribution of *JAK2* VAF in patients with or without additional somatic mutations. E) Clonal architecture determined by single colony genotyping in 11 MPN patients carrying multiple somatic mutations. Y-axis indicates the percentage of the colonies with or without the corresponding somatic mutations. The order of events depicted was deduced from the single clone analysis at one time point only.

Supplemental Figure S9

A Schematic illustration of a linear model for cell division dynamics

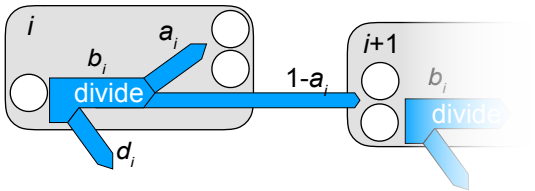

$$\dot{x}_i = 2b_{i-1}(1 - d_{i-1})(1 - a_{i-1})x_{i-1} - b_i d_i x_i - b_i(1 - d_i)(1 - 2a_i)x_i$$

a = self-renewal probability
b = division rate
d = probability of death
i = cellular compartment
x_i = number of cells in i

B Effects of altering division rate, b_i

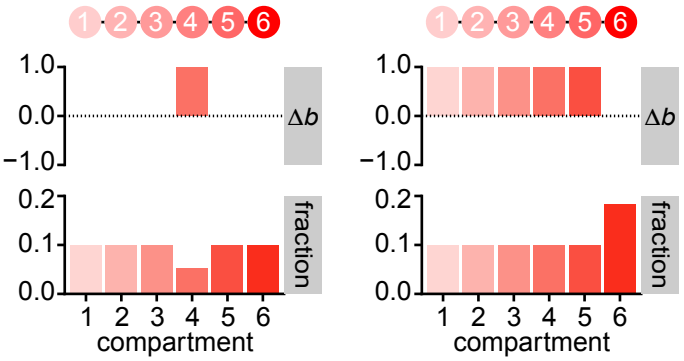

C Effects of altering death rate, d_i

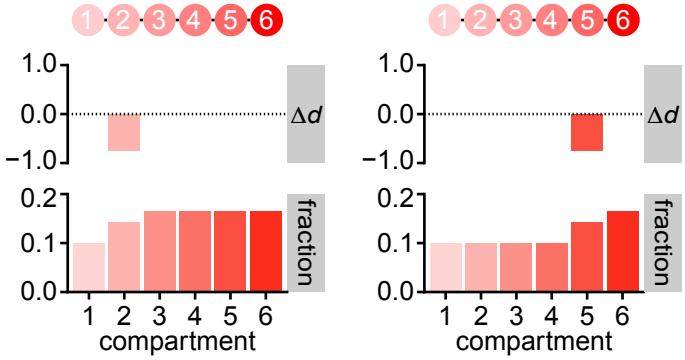

D Effects of altering self-renewal probability, a_i

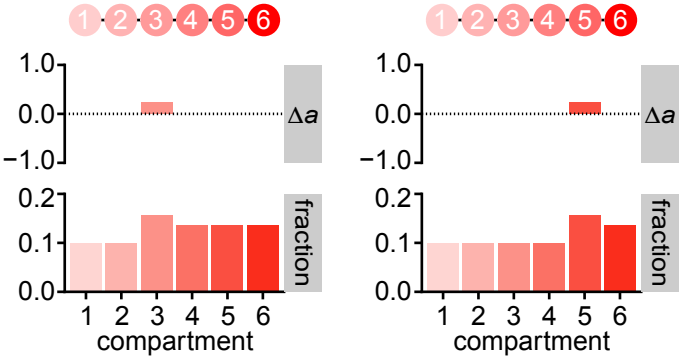

E Kinetics of clonal expansion in a branched population structure

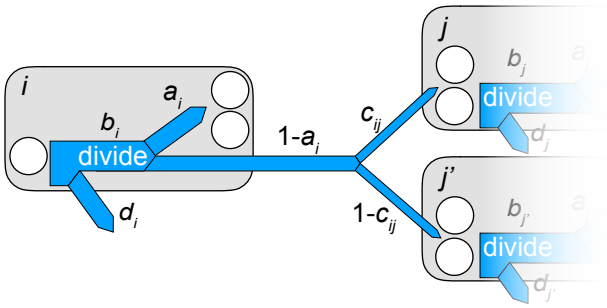

$$\dot{x}_i = 2\sum_j b_j(1 - d_j)(1 - a_j)c_{ji}x_j - b_i d_i x_i - b_i(1 - d_i)(1 - 2a_i)x_i$$

a = self-renewal probability
b = division rate
c = lineage bias
d = probabilty of death
i, j, j' = cellular compartment
x = compartment size

F Effects of lineage bias, c_{ij}

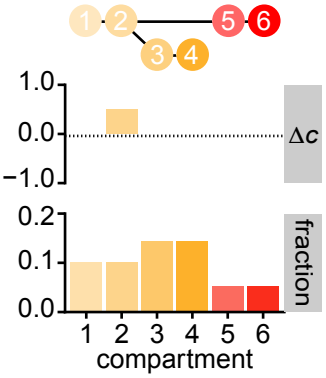

Supplemental Figure S9: Mathematical modeling of the individual parameters
We first modeled the effects that changes in individual parameters would have in a linear single lineage structure (A-D). The model (A) predicts that increasing the mutant cells' division rate solely at one stage of hematopoietic development will decrease the variant allele fraction (VAF) at this specific stage (B, left panel). A late clonal expansion at the final stage would result from increasing the division rate b in all preceding compartments (B, right panel). Such a situation increases the number of mutant cells flowing through the system, and then accumulating when they become terminally differentiated and stop dividing. Decreasing the death rate d at any stage leads to an increase in the VAF in this compartment, and a greater increase in the downstream compartments (C, left panel). Thus a lower death rate in the penultimate compartment could be observed as a late clonal expansion in the final two stages of development (C, right panel). Increasing the self-renewal probability a solely at one specific stage will increase the VAF in that compartment, plus in all subsequent compartments (D, left panel). A late clonal expansion could then be observed if there is greater amplification between the final compartment and its immediate progenitor (via a transient cell type between, e.g., the BFU-E and reticulocyte compartments; D, right panel). Since hematopoiesis is not a linear process, population branching is an additional source for altering VAF across the different lineages. Here we introduced an additional parameter, the lineage bias c_{ij}, that determines how the differentiated offspring of a multipotent cell are distributed across the different lineages (E). If the mutant cells have a bias towards a certain lineage, then the VAF will increase within that branch (F).

Supplemental Figure S10

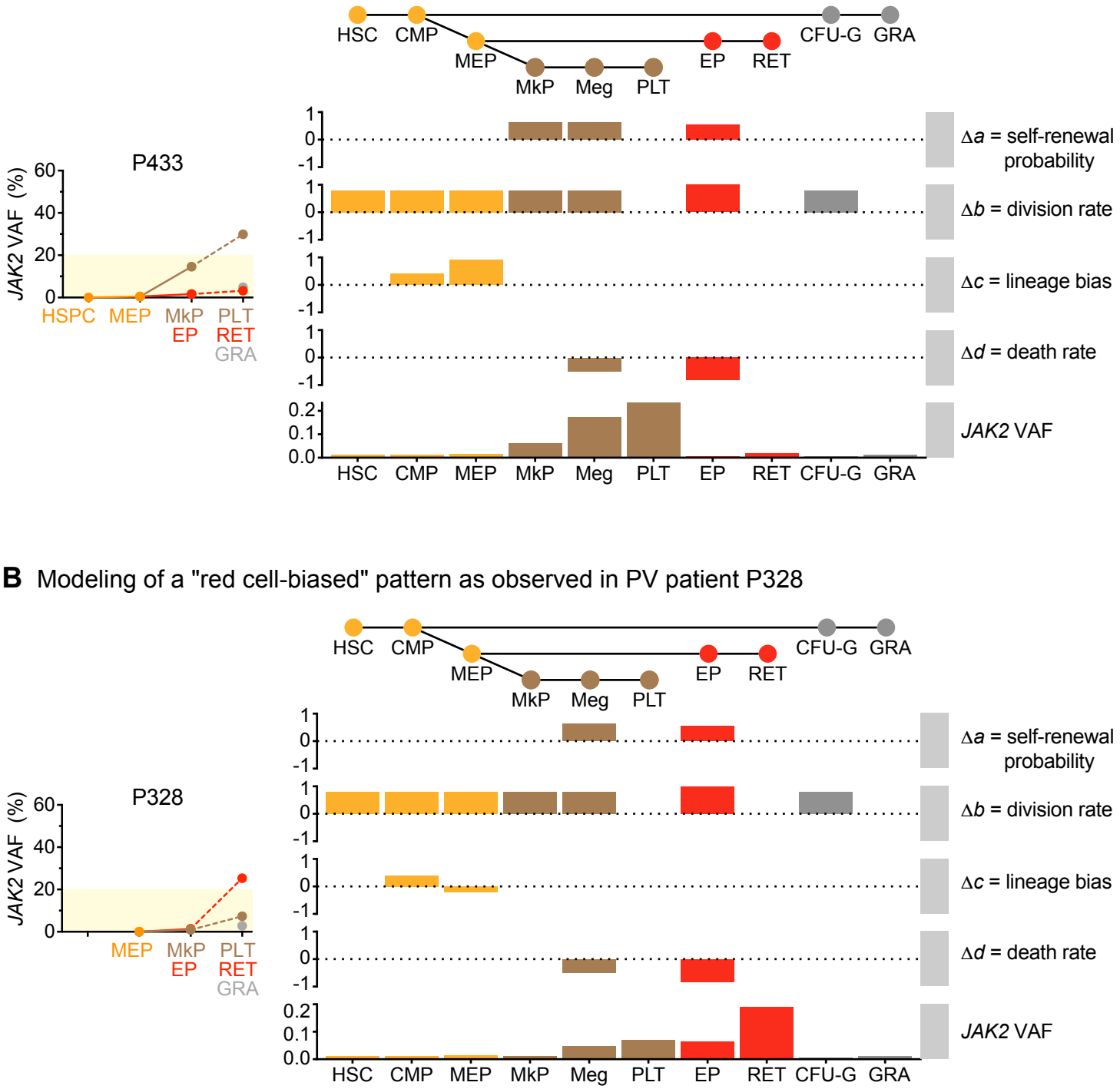

Supplemental Figure S10: Modeling of two individual cases with single lineage expansion. A) "Platelet-biased" pattern as observed in ET patient P433, B) "Red cell-biased" pattern as observed in PV patient P328. HSC, hematopoietic stem cell; CMP, common myeloid progenitor; MEP, megakaryocyte erythrocyte progenitor; MkP, megakaryocyte progenitor; Meg, megakaryocyte; PLT, platelet; EP, erythroid progenitors; RET, reticulocyte; CFU-G, colony-forming unit granulocyte; GRA, granulocyte; VAF, variant allele fraction